Electron-phonon coupling in high-pressure Nb

John S. Tse, Zhiqiang Li, Kentaro Uehara, and Yanming Ma*
Steacie Institute for Molecular Sciences, National Research Council of Canada, Ottawa, Ontario, Canada K1A 0R6

Rajeev Ahuja
Condensed Matter Physics Group, Department of Physics, University of Uppsala, Uppsala, Sweden
(Received 27 November 2003; published 21 April 2004)

The Fermi surface, phonon spectrum, and electron-phonon coupling parameter for metallic Nb under high pressure have been investigated with a full potential linearized augmented plane wave, linear muffin-tin orbital, and pseudopotential plane-wave methods. The results support the experimental observation of electronic topological transitions at 5 and 60 GPa. The lower pressure transition is related to a very subtle change in the topology of the Fermi surface as revealed in accurate calculations of the Hall coefficient. The transition at 60 GPa is identified with a change in the Fermi-surface topology due to the crossing of the electronic band along the $\Gamma \rightarrow N$ (Σ) direction in the cubic Brillouin zone. The calculated electron-phonon coupling parameters are in qualitative agreement with those derived from high-pressure experiment.

DOI: 10.1103/PhysRevB.69.132101 PACS number(s): 62.50.+p, 63.20.Kr, 74.70.Ad

Nb is the prototypical *d*-band metallic superconductor for which the mechanism for superconductivity at ambient pressure is believed to be well understood by theory.[1] Recently, under high pressure, the superconducting critical temperatures T_c were found to show anomalies at 5–6 GPa and 60–70 GPa, but no apparently structural changes.[2] A change in T_c is often associated with a modification of electron density of states at the Fermi level that is often the result of changes in the Fermi-surface topology. The anomaly observed at 5–6 GPa during quasihydrostatic compression has been interpreted[2] to the disappearance of the neck formed by the open sheet extending from $\Gamma \rightarrow H$ and the ellipsoids centered at *N* in the third extended Brillouin zone (BZ). However, this assertion apparently contradicts previous theoretical calculations at ~6 GPa and 26 GPa,[3,4] which predicted no significant changes in the Fermi-surface topology. The T_c anomaly that occurs near 60–70 GPa under a nonhydrostatic condition (no pressure medium) was assigned to the decrease of electron density states when the dip at Σ_1 along $\Gamma \rightarrow N$ (Σ) direction disappears at high pressure. Obviously, the Fermi-surface topology of Nb at high pressure is a fairly complicated issue and lacks a fundamental understanding.[5,6] The purpose of this paper is to investigate the Fermi surface and the electron-phonon coupling in Nb at high pressure using first-principles computational techniques.

Electronic band structure and Hall coefficient calculations were performed with the full potential linearized augmented plane-wave (FPLAW) method,[7] and electron-phonon coupling parameters were calculated with full potential linear muffin-tin orbital[8] (LMTO) and pseudopotential plane-wave[9] (PW) methods. For metal having cubic symmetry, the Hall coefficient in the low magnetic field limit is given by the following expression,[10]

$$R_H = \frac{\sigma_H}{\sigma_0^2}, \tag{1}$$

$$\sigma_H = \frac{e^3}{3\hbar} \int d\varepsilon \, \tau^2(\varepsilon, T) N(\varepsilon) \vec{v}(\varepsilon) [\mathrm{Tr}(\vec{M})^{-1} - \vec{M}^{-1}] \vec{v}(\varepsilon) \times \left[\frac{\partial f(\varepsilon)}{\partial \varepsilon} \right], \tag{2}$$

$$\sigma_0 = \frac{e^2}{3\hbar} \int d\varepsilon \, \tau(\varepsilon, T) N(\varepsilon) v^2(\varepsilon) \left[- \frac{\partial f(\varepsilon)}{\partial \varepsilon} \right], \tag{3}$$

where e, τ, f, M^{-1}, and v represent the charge of the electron (sign is included), the electronic relaxation time, the Fermi distribution function, the inverse mass tensor, and Fermi velocity, respectively. The inverse mass tensor is defined as

$$M_{xy}^{-1} = \frac{1}{\hbar^2} \frac{\partial^2 \varepsilon}{\partial x \partial y}, \tag{4}$$

which involves the second derivative of electronic band dispersion and is a very sensitive parameter to monitor small changes in the Fermi-surface topology.

If we assume an isotropic relaxation time, i.e., $\tau(\mathbf{k}, T) = \text{const}$, the Hall coefficient can be obtained directly from the band-structure results without resorting to the calculation of the anisotropic $\tau(\mathbf{k}, T)$ term. An accurate estimate of the Fermi-surface integration requires a very fine **k**-point mesh, and typically 70 000 **k** points were used in the first Brillouin zone. The calculated Hall coefficient for Nb at ambient pressure using FPLAW is 6.4×10^{-11} m^3/C which can be compared with the measured value of 8.72×10^{-11} m^3/C. Details of the numerical implementation of Fermi-surface interpolation and the Bloch tetrahedron integration scheme have been given elsewhere.[11]

The electron-phonon coupling parameters were calculated by the full-potential LMTO density-functional perturbation theory method.[8] In essence, the phonon linewidth γ_{qj} is calculated from the perturbed self-consistent field (SCF) potential. The spectral function $\alpha^2 F(\omega)$ is then evaluated and the electron-phonon coupling parameter λ is obtained from the

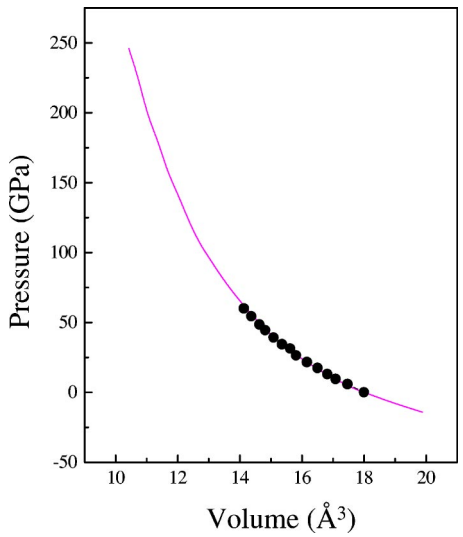

FIG. 1. (Color online) Comparison of calculated (line) and experimental (filled circles) equations of state for bcc Nb.

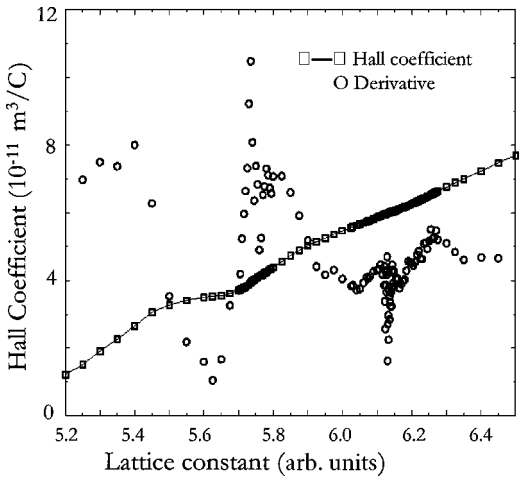

FIG. 2. Calculated Hall coefficient of bcc Nb and its derivative versus lattice constants.

k-space integration of the spectral function over the BZ. Convergence in **k**-point sampling is therefore crucial to the accuracy of the integration. We followed the procedure given in Ref. 8: the **k** integration for the construction of the induced charge density and the dynamical matrix is performed over a $16\times16\times16$ grid which is twice denser than the grid of the phonon wave vectors **q**. The **k**-space integration for the phonon linewidth is performed with a larger $32\times32\times32$ grid. In order to make meaningful comparison of the calculated electron-phonon parameter λ of Nb over the pressure range from ambient to 150 GPa, a smaller muffin radius was used. The presented calculated λ at the theoretical equilibrium volume is 1.36 which compares reasonably well with the experimentally derived value of 1.26 at $V/V_0=0.972$.[8] To check the reliability of the electron-phonon coupling parameters, particularly at the low pressure regime, linear-response calculations were performed using a pseudopotential PW method[9] employing the generalized gradient approximation[12] and a Troullier-Martins[13] norm-conserving pseudopotential. The kinetic energy cutoff was 40 Ry. and a $16\times16\times16$ Monkhorst-Pack grid was used in the SCF calculations, and a finer $32\times32\times32$ k point grid was used in the electron-phonon coupling calculations employing 28 **q** points in the BZ integration.

The equation of state (EOS) calculated from the FLAPW results is compared with the experimental measurement[14] in Fig. 1, and the agreement is quantitative. The electronic band structures for bcc Nb at 0, 50 and 150 GPa are shown in the top panel of Fig. 3. In agreement with previous studies,[3,4] no substantial modification of the Fermi surface is observed at low pressure below 50 GPa but there are minor changes along the $\Gamma\rightarrow N$ (Σ) and $N\rightarrow H$ symmetry directions. The dip almost touching the Fermi level along Σ at zero pressure is now lower than the Fermi level and the pocket along $N\rightarrow H$ has widened. These changes are reflected in the topology of the Fermi hole in the third zone (Fig. 3, bottom panel); in particular, the two ellipsoids are closer together at 50 GPa. These small changes in the Fermi surface have a subtle effect on the transport coefficient. The calculated Hall coefficient as a function of the lattice constant is shown in Fig. 2. A very small ''kink'' is observed at a unit-cell constant $\sim6.1a_0$ (bohr). To confirm this observation, the numerical derivative of the Hall coefficient with respect to the unit-cell size is evaluated employing much denser calculated points around $6.1a_0$. It is unmistaken that there is a discontinuity in the derivative curve. This discontinuity signifies a change in the electronic transport properties of the metal. Incidentally, the calculated pressure at this kink is 5 GPa, very close to the first anomaly in T_c observed in the experiment. A second, more distinctive discontinuity in the Hall coefficient is predicted at a unit-cell size that equals $5.72a_0$, which corresponds to a pressure of ~60 GPa. This change is clearly reflected in a significant modification of Fermi-surface topology. The calculated band structure at a unit-cell size of $5.54a_0$, which is slightly smaller than the transition at $5.72a_0$, shows substantial changes in the Fermi surface. Specifically, a pocket is now opened at Γ which extends along the $\Gamma\rightarrow N$ direction. A second pocket has developed around Γ and extends along the $\Gamma\rightarrow H(\Delta)$ direction. The Fermi hole topology shows the connecting of the two ellipsoids at Γ and a hole appears in the $\Gamma\rightarrow N$ direction. The substantial modification of the electronic density of states at the Fermi level is likely to be responsible for the T_c anomaly observed at 60–70 GPa.

To investigate the effects of the change in electron topology [electronic topology transition ETT] on the superconducting mechanism, the electron-phonon coupling parameters are computed as a function of the unit-cell size using both the LMTO and PW methods. The calculated density dependence of the electron-phonon coupling parameter λ is shown in Fig. 4. The general trend that the electron-phonon coupling parameter decreases with increasing density (or pressure) is well reproduced by both methods. This profile is in good agreement with the λ values estimated from experimental T_c using the Allen-Dynes modification[15] of McMillan equation[1] for T_c. Under quasihydrostatic compression con-

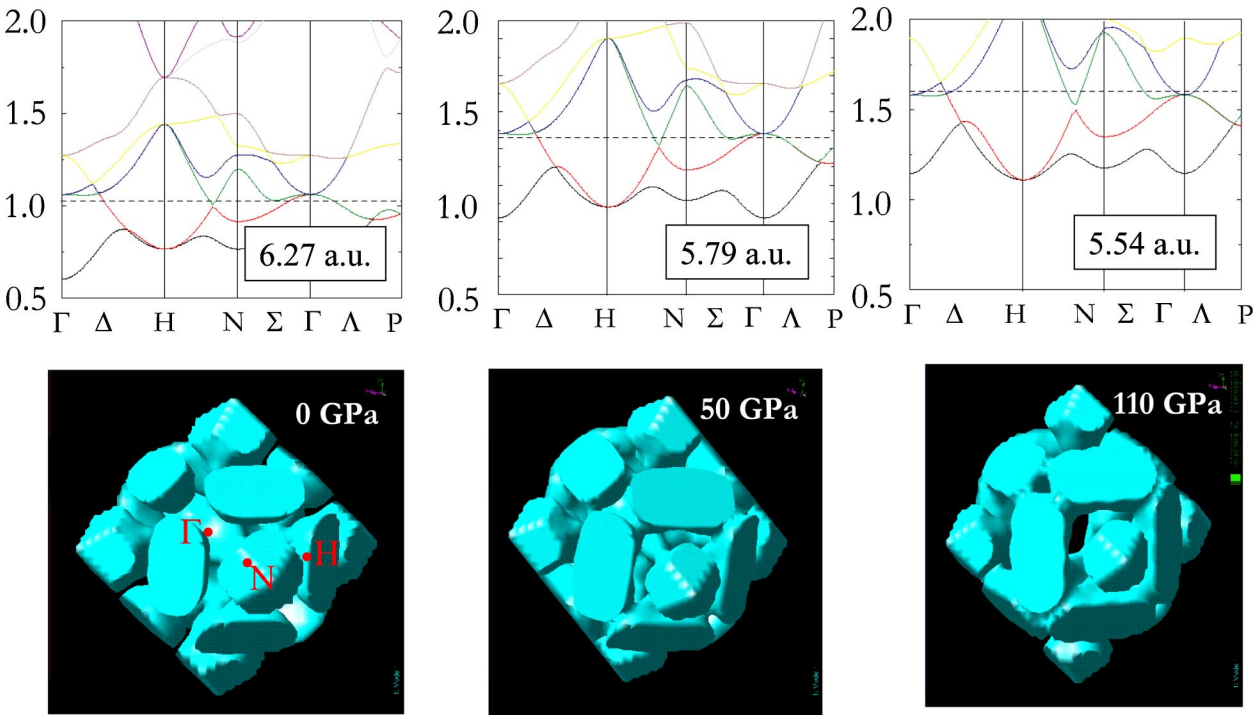

FIG. 3. (Color online) Electronic band structure (in eV) and the Fermi surface of bcc Nb at several pressures.

ditions, the experimentally derived λ first shows a decrease from the ambient value of 1.16 to 1.12, then a sudden rise to 1.18 at $\rho/\rho_0=1.02$, and then decreases smoothly to 1.04 at $\rho/\rho_0=1.32$. For compression without a pressure transmission medium, the T_c shows an abrupt decrease at ~60 GPa. This abrupt change is echoed in a slight change of slope at $\rho/\rho_0=1.32$ in the derived λ.

Two distinct discontinuities are predicted at $\rho/\rho_0=1.02$ and 1.27 (see the arrows in Fig. 4), corresponding to lattice constants of $6.17a_0$ and $5.72a_0$ and a calculated pressure of 5 and 60 GPa, respectively although the discontinuity at 5 GPa calculated from the PW method is not as prominent as in the LMTO calculations. In agreement with the experimentally derived λ, at low pressure the LMTO calculated electron-phonon coupling parameter decreases from 1.36 to 1.02 and then increase sharply to 1.21 at $\rho/\rho_0=1.02$ or 5 GPa. The electron-phonon coupling then decrease smoothly to about 0.98 at $\rho/\rho_0=1.25$. Riding on the gradually decreasing λ the calculation shows a broad peak centered at $\rho/\rho_0=1.28$ where the coupling parameter increases slightly from 0.98 to 1.19. Although, an anomaly in λ is correctly predicted at the appropriate pressure range, and therefore the superconducting critical temperature T_c, the theoretical profile differs from that of the derived λ. This discrepancy may not be too surprising since several assumptions were invoked in the estimation of λ from the measured T_c. In particular, the assumption of a smoothly varying Slater-Gruneisen parameter with pressure may not be appropriate at the phase transition where the Fermi-surface topology and the phonon frequencies changed significantly. A smaller $\omega_{\log}$, due to phonon softening at the electronic topological transition, will lead to a larger estimate of λ, bringing the derived electron-phonon coupling parameters into a better agreement with theoretical predictions.

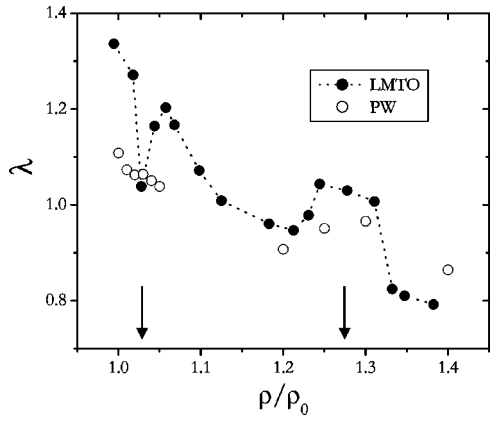

FIG. 4. The density dependence of the electron-phonon coupling parameter for bcc Nb calculated with full potential LMTO and pseudopotential PW methods. The dotted line through the LMTO results is for a guide.

The interpretation of the calculated ETTs differs from that proposed based on the experimental findings.[2] The low-pressure anomaly observed at 5 GPa is shown to be due to slight changes in the Fermi surface along the $N\rightarrow H$ and extends to $\Gamma\rightarrow H$. The more prominent ETT transition observed at 50–60 GPa is attributed to the moving down of the energy band (Γ'_{25}) (Ref. 2) around Γ and opening pockets along the $\Gamma\rightarrow N$ and $\Gamma\rightarrow H$ directions.

In conclusion, the present theoretical investigation of the

transport coefficients and the electron-phonon coupling parameters of bcc Nb under pressure confirm the occurrence of two ETT transitions at 5 and 60 GPa. These ETTs have notable effects in the electron-coupling parameter and affect the superconducting T_c. Moreover, since isotropic compression is implicitly assumed in the calculations, therefore, nonhydrostatic uniaxial stress is not responsible for the anomaly in T_c observed at 50–60 GPa.[2]

*Permanent address: National Lab of Superhard Materials, Jilin University, ChangChun 130012, People's Republic of China.

[1] W. L. McMillan, Phys. Rev. **167**, 331 (1968).
[2] V. V. Struzhkin *et al.*, Phys. Rev. Lett. **79**, 4262 (1997).
[3] J. R. Anderson, D. A. Papaconstantopoulos, J. W. McCaffrey, and J. E. Schirber, Phys. Rev. B **7**, 5115 (1973).
[4] J. R. Anderson, D. A. Papaconstantopoulos, and J. E. Schirber, Phys. Rev. B **24**, 6790 (1981).
[5] A. K. Solanki, R. Ahuja, and S. Auluck, Phys. Status Solidi B **162**, 497 (1990).
[6] A. K. Solanki, R. Ahuja, and S. Auluck, Phys. Status Solidi B **182**, 377 (1994).
[7] P. Blaha, K. Schwarz, and J. Luitz, WIEN97, improved and updated Unix version of the original copyrighted WIEN code, which was published in Comput. Phys. Commun. **59**, 399 (1990).
[8] S. Y. Savrasov and D. Y. Savrasov, Phys. Rev. B **54**, 16487 (1996).
[9] S. Baroni, P. Giannozzi, and A. Testa, Phys. Rev. Lett. **58**, 1861 (1987); P. Giannozzi, S. de Gironcoli, P. Pavone, and S. Baroni, Phys. Rev. B **43**, 7231 (1991); S. Baroni, A. Dal Corso, S. de Gironcoli, and P. Giannozzi, http://www.pwscf.org.
[10] J. M. Ziman, *Principles of the Theory of Solids* (Cambridge University Press, London, 1964).
[11] K. Uehara and J. S. Tse, Phys. Rev. B **61**, 1639 (2000).
[12] J. P. Perdew and K. Burke, Int. J. Quantum Chem. S **57**, 309 (1996); J. P. Perdew, K. Burke, and M. Ernzerhof, Phys. Rev. Lett. **77**, 3865 (1996).
[13] N. Troullier and J. L. Martins, Phys. Rev. B **43**, 1993 (1991).
[14] K. Takemura (private communication).
[15] P. B. Allen and R. C. Dynes, Phys. Rev. B **12**, 905 (1975).